J. Astrophys. Astr. (2002) **23,** 243–258

Spectral Variability in Hard X-rays and the Evidence for a 13.5 Years Period in the Bright Quasar 3C273

R. K. Manchanda *Tata Institute of Fundamental Research, Colaba, Mumbai 400 005, India*
e-mail: ravi@tifr.res.in

Received 2002 October 21; accepted 2002 December 12

Abstract. We report the observation of nearest quasar 3C273 made with LASE instrument on November 20th, 1998 as a part of our continuing programme of balloon borne hard X-ray observations in the 20–200 keV band using high sensitivity Large Area Scintillation counter Experiment. Our data clearly show a steep spectrum in the 20–200 keV with power law spectral index $\alpha = 2.26 \pm 0.07$. This is in complete contrast to the reported data from OSSE and BeppoSAX which suggest the value of 1.3 to 1.6 for the power law index in the X-ray energy band, but is quite consistent with the value derived for the high energy gamma ray data. A single power law fit in the X-ray and gamma ray energy bands points to a common origin of these photons and the absence of spectral break around 1 MeV as suggested in literature. We have reanalyzed the available data to study the temporal variability of the spectrum in the hard X-ray band. Our analysis reveals that 50 keV flux from the source, shows a strong modulation with a period of about 13.5 years. The analysis of the optical light curve of the source also supports the 5000 day period. We discuss the emission mechanism and the possible sites for X-ray photons along with the implications of the long term periodicity with respect to source geometry.

Key words. Galaxies: active galactic nuclei, jets, binary black hole system—quasars: individual 3C273—X-rays: galaxies.

1. Introduction

Among the large variety of active galactic nuclei, 3C273 is the nearest quasi stellar object with red shift $z = 0.158$. The source has been studied in detail in various energy bands and shows a large variety of morphological features. These include, a continuously fuelled curved inner jet with superluminal components observed in VLBI observations (Davis, Muxlow & Unwin 1991), an outer jet which is also visible in radio and optical wavelength other than the X-ray band and the UV excess (blue bump). The multiband spectrum of the source extends from radio to the GeV gamma rays region (Courvoisier *et al.* 1987) and can only be compared with the Crab Nebula, which also emits in the entire observable band. The spectral energy density distribution in 3C273 shows two broad peaks in the UV region (~ 10 eV) and the gamma ray energy band of 1–10 MeV (Ramos *et al.* 1997).

The X-ray emission from 3C273 in the soft X-ray band of 2–10 keV was first detected by Boyer *et al.* (1970). Since then the spectral observation of the source has been made in the X-ray and gamma ray energy bands, not only by balloon borne instruments (Pietsch *et al.* 1981; Bezler *et al.* 1984; Damle *et al.* 1987; Dean *et al.* 1990; Maisack *et al.* 1989, 1992) but also, by every X-ray payload launched on satellite missions till date i.e., HEAO-1 (Worrell *et al.* 1979; Primini *et al.* 1979), Einstein (Wilkes & Elvis 1987), SIGMA/GRANAT (Bassani *et al.* 1992), Ginga (Williams *et al.* 1992), ROSAT (Leach, McHardy & Papadakis 1995), EXOSAT (Turner *et al.* 1995) and ASCA (Cappi & Matsuoka 1997). The broadband data were obtained by OSSE (Johnson *et al.* 1995), COMPTEL (Hermsen *et al.* 1993) and EGRET (von Montigny *et al.* 1993) detectors on board CGRO and BeppoSAX (Grandi *et al.* 1997).

A temporal variability of the continuum emission from 3C273 in different energy bands is a regular feature of the source and has been discussed in literature (Courvoisier *et al.* 1987). Below 10 keV, the X-ray spectrum does show a large change in the spectral index on occasions, and can be fitted by a two component model in addition to a variable intensity weak and narrow Fe K_α emission line (Cappi & Matsuoka 1997). In the hard X-ray energy region of 20–200 keV, the spectrum generally follows a power law with a spectral index close to 1.5 however, a much steeper power index of 2.2 has also been reported in the archival data. The recent data from OSSE and BeppoSAX experiments show the canonical spectrum with index $1.4 < \alpha < 1.6$ except for a single observation of a flat spectrum with index 0.8 when the source intensity was lower by a factor of ~ 3. It was also noted from the Ginga data that the hard X-ray spectrum does not show any correlation with the flux variation in the 2–10 keV band. In the gamma ray energy band of 1 MeV to 1 GeV, the best fit spectral index is 2.4 (Litchi *et al.* 1994). From a comparison of the contemporary observations of the source made with the OSSE, COMPTEL and EGRET instruments, Johnson *et al.* (1995) have proposed a break in the source spectrum at around 1 MeV and steepening of the power index by ~ 1.

The X-ray emission in 3C273 is believed to arise by the synchrotron self Compton process (SSC) in the jets in which seed synchrotron photons are up scattered by interaction with the high energy electrons. X-ray and gamma ray emission in beamed relativistic jets in relation to BL Lac objects in general, and 3C273 in particular has been discussed in literature (Konigl 1981). The observation of soft X-ray excess below 1 keV in 3C273 and the flux variability below 10 keV, does suggest the presence of additional component which may arise from the thermal Comptonization of the soft photons originating in the accretion disc. The observation of the correlated variability in the medium energy X-rays and the K-band flux does however, suggest a generic relation between the two and a common emission process which also accounts for the bulk of X-ray photons emitted from the source (McHardy *et al.* 1999). The simultaneous multi-frequency observations in the radio and UV/Opt bands however, do not show a clear one-to-one correlation with the X-ray data (Ulrich *et al.* 1988).

The observed variability in the X-ray data of 3C273 is random and does not show any preferred time scales. ASM data on RXTE however, does show occasional flare like behaviour of the source. A $\sim 0.5\ d$ periodicity was first suggested from the Ariel 5 data (Marshall, Warwick & Pounds 1981). A comparison of the different data and the BATSE light curve in the 20–120 keV gives a variation in flux level by a factor ~ 2 over a period of months to years. A similar variation in the source flux over time scale of weeks was seen in the EXOSAT and Ginga data while the intensity variation by a factor of ~ 2 with a period of six months has been reported from the ROSAT data (Kim

2001). The observations of the source in the radio band show that new components are ejected into the inner jets ever since 2–4 years and thereby may result in the long term variation of the source. An existence of a 2 year period in the optical data of the source has been proposed by Fan *et al.* (2001). No definite periodic components have been found so far.

In this paper we report the hard X-ray spectral measurements of 3C273 made in the 20–200 keV band. The present measurements suggest that the entire X-ray and gamma ray emission from the source may arise in a single non-thermal process. We have re-analyzed the archival data by a new 'residual method' and conclude the presence of a long term variability of 13.5 years in the X-ray flux from the source. The re-analysis of the available optical data on the source also reveals the evidence of a similar long term period.

2. Present data

The spectral measurements were made during a balloon flight experiment using a large area scintillation counter telescope (LASE) operating in the 20–200 keV energy band. The X-ray telescope has a modular design and is optimized to make fast spectral and temporal measurement of cosmic X-ray sources in the hard X-ray band with very high sensitivity. The payload consists of three modules of scintillation detectors having both passive and active shielding and are fitted on a fully steerable alt-azimuth mount. Each of the three detector modules used in the experiment has a geometric area of 400 cm^2 and is specially configured in a back-to-back geometry. The field of view of each module is $4.5^\circ \times 4.5^\circ$ and is made with specially designed sandwiched material of tin, copper and lead. All modules have independent event-selection logic, onboard radioactive source calibration, PHA analyzer and the arrival time of the accepted events is recorded with a time resolution of 25 μsec. A 3σ threshold sensitivity of the LASE telescope in the entire energy range up to 200 keV is $\sim 1.5 \times 10^{-6}$ $cm^{-2}s^{-1}keV^{-1}$ for a source observation of 10^4 sec. The details of payload are given elsewhere (Manchanda 1998; D'Silva *et al.* 1998).

The observations were made on November 21st, 1998 from Hyderabad, S. India. The source observations were preceded and followed by off-source measurement from a nearby source free region. The total number of excess counts due to the source in all three detectors were 12418 during the source observation of 3540 sec and corresponds to a combined statistical significance of 20σ in the 35 to 160 keV energy band. The excess count rate spectrum was computed for the source and then corrected for the atmospheric absorption including multiple Compton scattering effects, window transmission and detector response functions. The spectra from all the three detectors were co-added. The observed photon spectrum is shown in Fig. 1. A single power law fit of the form $\frac{dN}{dE} = K\, E^{-\alpha}$ ph. $cm^{-2}s^{-1}keV^{-1}$ to the spectral data above 35 keV gives the best fit model parameters of $K = 0.7$ and $\alpha = 2.26 \pm 0.07$ with a reduced χ^2 value of 0.2 corresponding to 7 degrees of freedom. The power law fit is shown in the figure with solid line. The data shown in the figure suggest a residual excess over the best fit line at about 120 keV, however, the total significance of the this feature is only $\sim 2\sigma$. It is also seen in the figure that high statistical significance of the individual data points for energies below 80 keV control the spectral index of the power law fit. The present observations correspond to MJD 2451137.

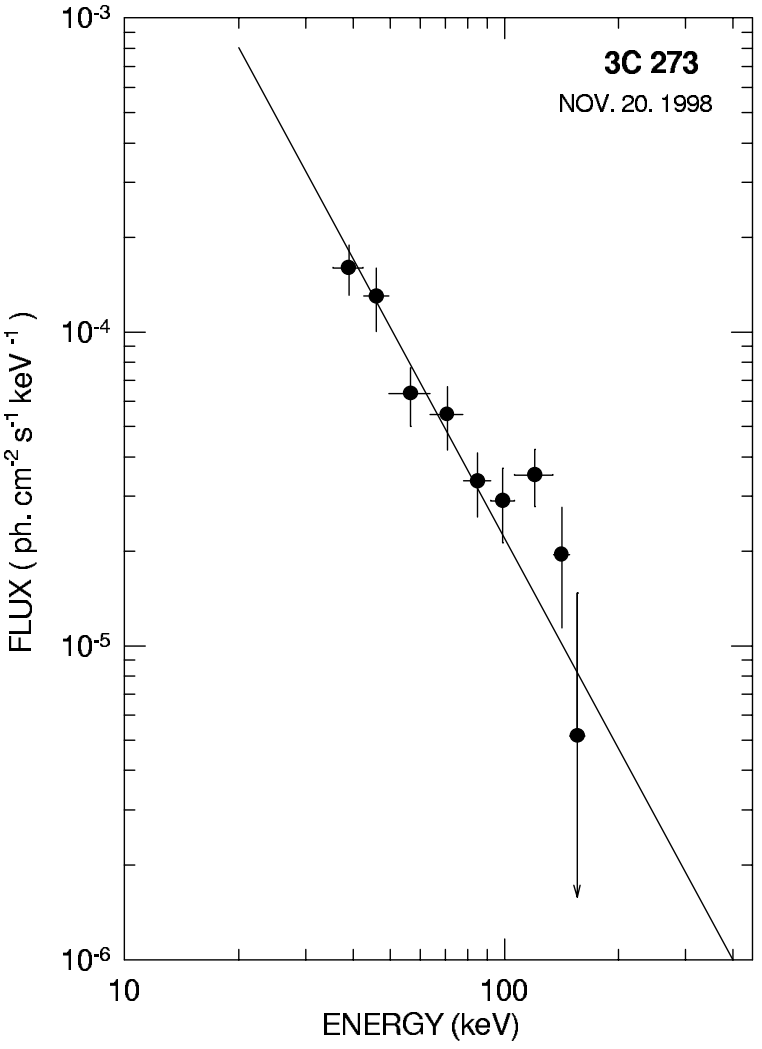

Figure 1. Hard X-ray spectrum of 3C273.

To determine the activity level of 3C273 corresponding to the spectral data presented above, and to illustrate the long term temporal behaviour of the source, we have plotted X-ray light curves taken from the archival data in Fig. 2. The left panel in the figure shows the X-ray light curve of the source from BATSE data on board CGRO in the 20–120 keV band. The all sky monitor data on-board RXTE in the 2–6 keV band is shown in the right panel. It is seen from the figure that in the hard X-ray band the source intensity does show gradual variation in intensity over long time scales and the source is clearly detectable even in the quiescent or normal phase. In the soft X-ray band however, the X-ray emission does show flare like behaviour on several occasions as is evident from the ASM data (right panel). It is also seen from the figure that present observations correspond to the normal state of the source.

A comparison of the present results with the earlier data in the hard X-ray ray band up to 300 keV is shown in Fig 3(a). The data shown in the figure correspond to the

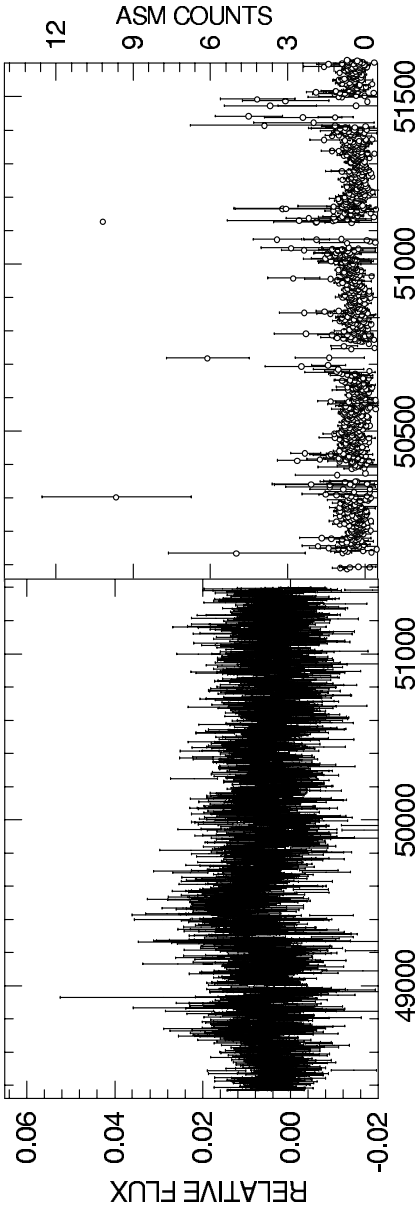

Figure 2. X-ray light curve of 3C273 as seen in BATSE (left panel) and RXTE data.

observations by SIGMA-Granat mission (Bassani *et al.* 1992), MIFRASO data (Dean *et al.* 1990) and OSSE detector on-board Compton/GRO observatory (Johnson *et al.* 1995). It is seen from the figure that present values of spectral flux in various energy bins is consistent with the SIGMA and MIFRASO data. The two dotted lines in the figure represent the high state and the low state spectra from OSSE data. It is seen in the figure that the present data is consistent with the high-state spectrum of the source from OSSE while the low state spectrum does vary significantly. The best fit power law index obtained from the present observations is also consistent with the data in the gamma ray energy region up to 10 GeV and is shown in Fig. 3(b). The gamma ray data in the figure corresponds to the observations made by COMPTEL and EGRET telescope (Hermsen *et al.* 1993, von Montigny *et al.* 1993). This in turn suggests a common emission mechanism for the high energy X-rays and gamma ray photons.

3. Spectral variability in hard X-rays

The compilation of the world data shown in Fig. 3, does appear to be consistent globally and the large scatter in the measured flux values at any given energy can be ascribed to the temporal variability as shown in Fig 2. However, when considered individually, the value of the measured spectral indices shows a large variation between 1.2 ± 0.17 and 2.26 ± 0.07. In order to find any correlation between the observed source luminosity and the spectral index as well as deduce the periodic behaviour of the source spectrum, we have devised the 'residual analysis' for the individual data sets. We have used the present measurement as the spectral template. The residuals are computed in each energy bin for different data and are shown in Fig. 4. We have split the world data in two parts i.e., pre and post 1983. In the case of earlier data the residuals were computed only at 50 keV and at 100 keV. The HEXE data are taken from Maisack *et al.* (1992). For convenience of plotting the data, the flux values were multiplied with $E^{-2.26}$. It is seen from the figure that data above 100 keV fit the mean spectra in all data sets thereby producing near zero residuals. Below 100 keV, high and low residuals are seen in different data sets. In the composite panel of pre 1983 data, once again the variability in the individual data sets is clearly visible. This analysis therefore, illustrates the possible spectral variability in 3C273 and that the observed variations are confined to energies below 100 keV in the hard X-ray region. This in turn suggests a two component origin for the hard X-ray photons, one of which exhibits temporal variations.

4. Long term periodicity in the source

In order to derive the long term period in 3C273, we have plotted the 50 keV flux (F_{50}) values as measured during different observations starting with the earliest measurements in Fig. 5. The choice of flux value at 50 keV is due to the fact that majority of the earlier measurements are made in balloon-borne observations and the systematic corrections are negligible at $\sim$ 50 keV. The pre 1990 compilation is taken from Bassani *et al.* (1992) and later high quality data corresponds to OSSE observations of the source. Apart from the short term variations, the data in the figure show a clear evidence of long term periodicity in the source. Assuming a sinusoidal functional form, an eye fit to the data gives a period of about 13.5 years ($\sim$ 5000 days). A similar plot

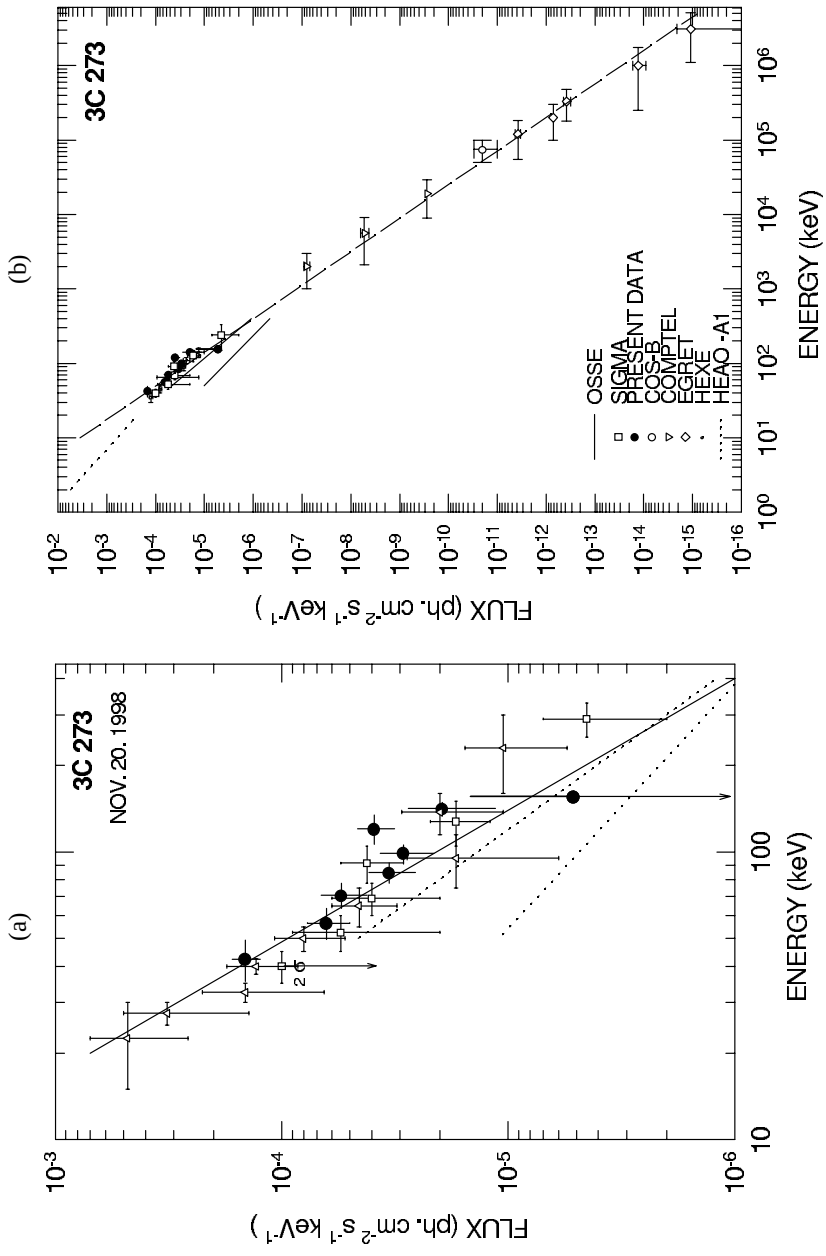

Figure 3. **(a)** Hard X-ray spectrum of 3C273. □ SIGMA, Δ MIFRASO, - - - OSSE, ● present data. Solid line, the best fit power law as in Fig. 1. **(b)** Photon spectrum in the entire X-ray and gamma ray energy band. The dotted line in the figure represents the extrapolation of best fit spectrum.

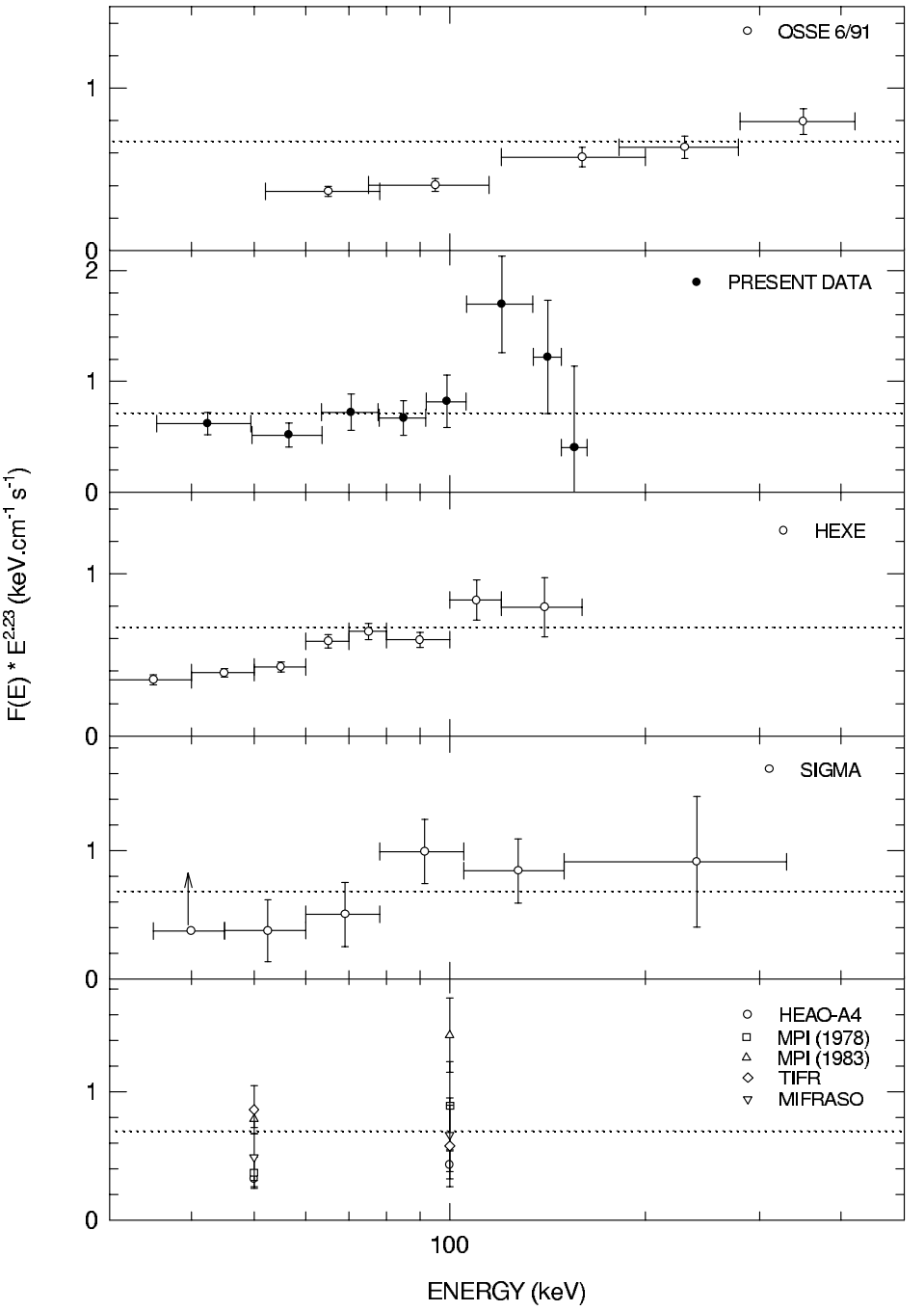

Figure 4. Plot for the spectral residuals for different data sets. Residuals are computed by taking $\alpha = 2.26$, as the best fit power index from keV to GeV energy band.

for the 100 keV flux, F_{100} did not show a clear period. Such a behaviour was expected on the basis of the variability plot shown in Fig. 4 in which the zero residuals were noted for data above 100 keV in all data sets. Similarly the long term periodicity is also not so apparent in the value of the spectral index as shown in the top panel in Fig. 5. The absence of long term period in the power law index can be ascribed to the emission mechanism for the hard X-ray photons and the temporal variation in the X-ray luminosity of the source. In addition, in a two component model, if the amplitude of the periodic component is small, the spectral index will remain mostly unchanged.

To search for additional evidence for the long term periodicity in 3C273 as inferred above, we have re-analyzed the optical brightness data of the source. The 110 year data base is due to Fan *et al.* (2001). The plot for the observed magnitude of the source versus modified Julian date is shown in Fig. 6 (left panel). The underlying long term variability can be clearly seen in the data. For searching the coherent periodicity in the optical data we used the XRONOS folding routine. The data were searched for periods between 3200 and 6000 days in 200 steps. The resultant power vs. period is shown in Fig. 6. (right panel). A broad peak centered around 4790 days is clearly visible in the figure. The large deviation of $\pm 205\ d$ in the determination of the period is due to short data base for long period searches. The presence of long term period in the optical data consistent with that inferred from the X-ray band clearly points to the true nature of the period.

5. Discussion

5.1 *Photon production and the emission sites*

A simple power-law nature of the spectrum in the entire X-ray and gamma ray region up to GeV as seen in figure 3, suggests a non-thermal origin for these photons and can arise either in pure synchrotron process or due to Synchrotron Self Compton process. The basic ingredient for this process to operate is the high energy relativistic electrons, which first give rise to the synchrotron seed photons and then up scatter these to higher energies in the case of SSC and if the seed photons have a power law spectrum, the emergent spectral index will be harder. In either of these processes a population of relativistic electrons is pre-requisite. The jets are the most suited geometry for the shock acceleration of the electron to very high energies. The detection of radio flux from the jets is itself an evidence of the presence of relativistic particles and *in situ* acceleration. The particle acceleration in the jets is believed to be due to shock wave at the interaction boundary of the expanding relativistic plasma and the ambient environment. During the shock acceleration a particle with velocity v gains a momentum $\simeq w/v$ every time it crosses the shock of velocity w. If the particles are scattered efficiently on both sides of the shock and stay trapped, the particle can reach relativistic energies provided the adiabatic losses are negligible. In case of the diffusive shock the maximum proton energy $E^p_{\max} \sim 10^{15}$ eV is attainable for a shock compression ratio of ~ 4 and reasonable values for other parameters (Mitra 1991). The shock acceleration of the particles transmits a power law spectrum and for a shock compression of $\sim$3–4 the exponent lies between 2 and 2.5.

The observed spectral energy density of 3C273 at higher energies is very large. Therefore, for Compton losses to be comparable to synchrotron energy loss the Lorenz factor for electrons, needs to be large compared with magnetic energy density. The

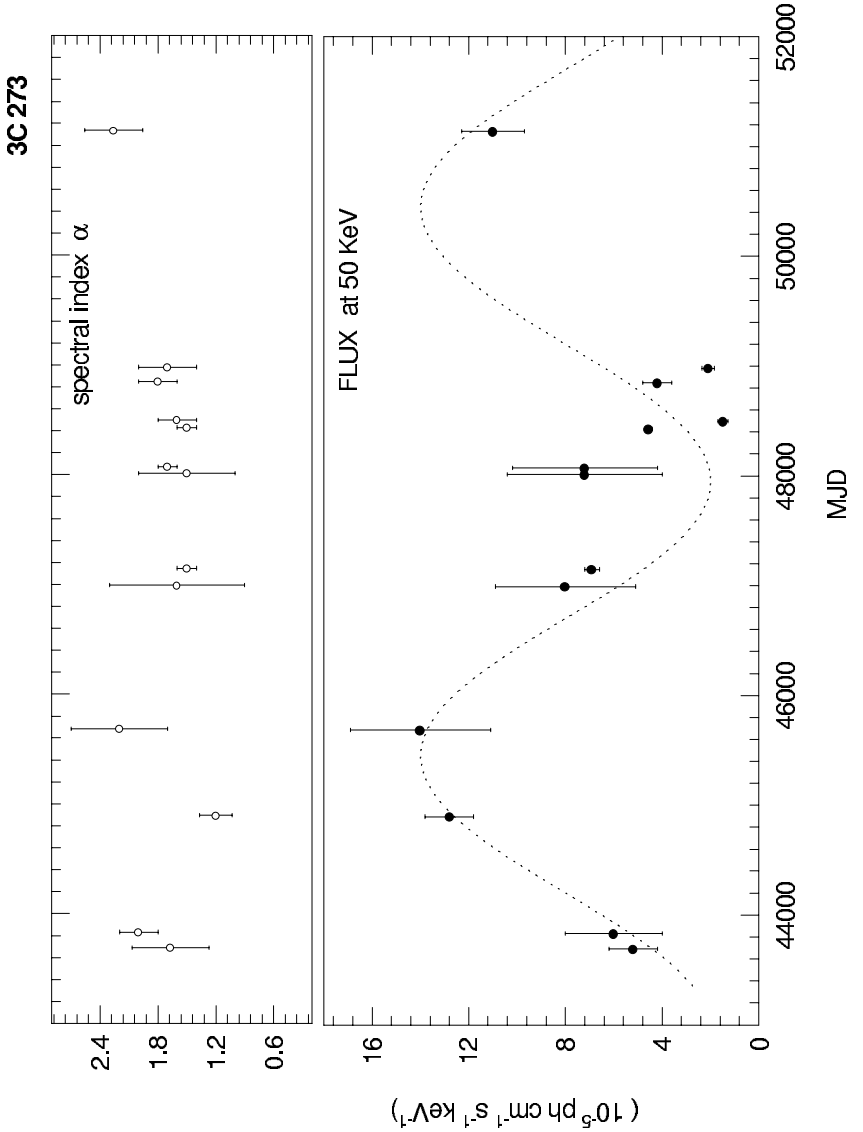

Figure 5. Long term variability of the X-ray flux from 3C273. The lower panel shows the measured flux values at 50 keV. Upper panel gives the best fit power law indices.

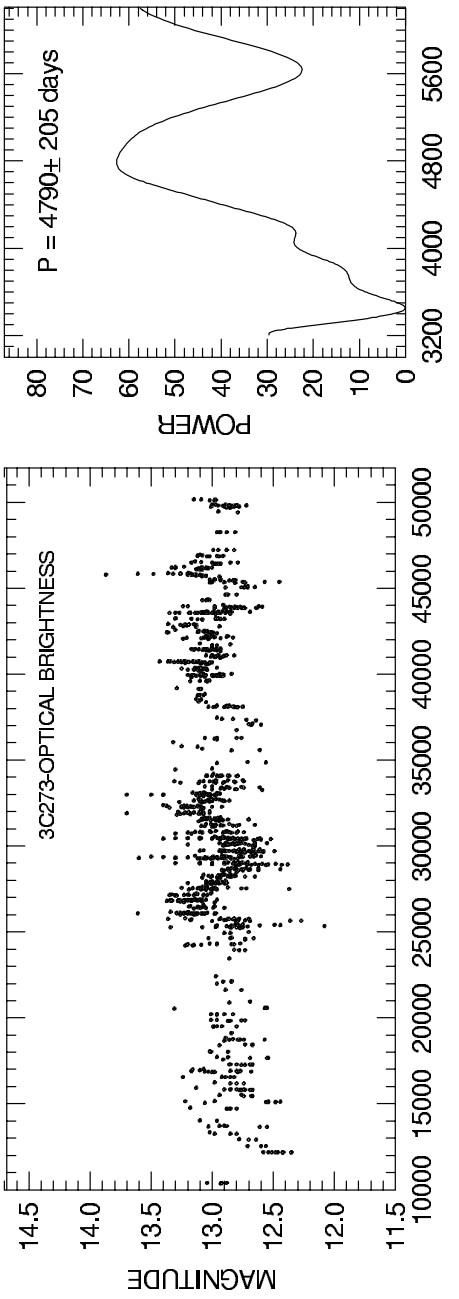

Figure 6. The optical light curve of 3C273 (left panel) and the periodogram obtained during the period analysis using XRONOS (right panel).

ratio of the energy losses of electrons in the synchrotron and synchrotron self Compton processes can be written as:

$$\frac{\dot{\gamma}_{\rm syn}}{\dot{\gamma}_{\rm ssc}} = \frac{B^2/8\pi}{\frac{1}{c}\int \mathcal{F}_\nu^{\rm syn} d\nu}$$

where the synchrotron luminosity $\mathcal{F}_\nu$ is given by (Ginzberg & Syrovatskii 1964);

$$\mathcal{F}_\nu \, d\nu = a'(\gamma)(e^3/mc^2)\left(3e/4\pi m^3 c^5\right)^{(\gamma-1)/2} \; (B_\perp)^{(\gamma-1)/2} L K_e \; \nu^{-(\gamma-1)/2} d\nu$$

for a power law electron spectrum of the form $N(E) = K_e \, E^{-\gamma}$ where $a'(\gamma) \sim 0.15$. For the SSC processes to operate successfully it is necessary to have magnetic field $B \leq 10^6 G$; which is an order of magnitude smaller than the inferred values. It is to be noted that photon emission from the jet requires a continuous injection of electrons into the jets and this can only take place if we assume a continuous flaring geometry as proposed in the case of Mkn 421 (Manchanda 2001). The gradual increase and decrease in the source flux over days to months is consistent with the jet emission model. A pure jet emission however, does not explain the large excess in the soft X-ray band below 1 keV and the occasional flare like behaviour observed in the ASM light curve of the source. Furthermore, the expected spectral energy distribution in the synchrotron or the SSC processes is a simple power law form while the observed distribution shows two broad peaks as noted earlier. In addition, the CHANDRA observations of the structure and the X-ray emission from the jet of 3C273 also suggest that in the soft X-ray region of 0.2–8 keV, only a part of the observed flux may be explained by the jet emission (Sambruna *et al.* 2001). The observation of a weak and a narrow Fe K_α line itself suggests the presence of an additional emission region in the source.

We therefore, propose that a photon emission arising from the accretion disk around the central black hole accounts for the remaining spectral features of the source. The temperature structure of a classical thin accretion disk is given by;

$$T^4 = \frac{3GM\dot{M}}{8\pi\sigma r^3}\left[1 - \left(\frac{r}{R_{\rm min}}\right)^{-1/2}\right]$$

and assuming that AGNs are accreting close to the Eddington rate with about 10% efficiency, the radial distribution of the temperature in the disk is given as:

$$T(r) \approx 6.3 \times 10^5 \left(\frac{\dot{M}}{M_{\rm edd}}\right)^{1/4} \left(\frac{M}{10^8 M_\odot}\right)^{-1/4} \left(\frac{r}{r_s}\right)^{3/4} {}^\circ K,$$

from which we expect a peak in the spectral energy distribution in the UV/soft X-ray region, which might in fact be the origin of the big blue bump seen in 3C273. The evidence for the accretions disks in AGNs is growing steadily i.e., the measurement of double peaked H_α profile in NGC 1097 (Storchi-Bergmann *et al.* 1997) and its variability can be interpreted as an evidence of the accretion disk and the binary nature of the central source similar to the observations in symbiotic stars. In fact, the simultaneity of the optical and UV flux in the case of AGNs suggests that these photons can not originate in the accretion process due to frequency dependence of the drift

time scales and therefore, must originate by the reprocessing of X-ray photons in the cold matter of the accretion disk, which is also consistent with the observed equivalent width of the 6.4 keV Fe K_α line in these sources. The disk like Fe K_α line profile seen in Seyfert 1 galaxies, which is believed to arise in the gas rotation at relativistic speed in the Keplerian accretion disk does support the irradiation model. Hence, the observed Fe emission line profile and the correlation between the medium energy X-ray photons and the IR photons in K band in 3C273 can easily be accomplished in a model in which the accretion disk is irradiated by the downward moving hard X-ray photons external to the disk.

We further suggest that the underlying photons spectrum with $\alpha \sim 2.4$ as seen at the gamma ray energies is the true representative of the jet emission arising in non-thermal process. The UV bump is caused by the hot accretion disk. While the iron line is formed due to external irradiation of the disk. Additional contribution to the medium and hard energy X-ray bands will arise due to thermal Comptonization of the large number of available seed photons in the hot plasma surrounding the disk. Up grading of the low energy photons in Compton collisions with thermal electrons has been discussed in the case of galactic black hole candidate Cyg X-1 (Sunyaev & Titarchuck 1980). The added photon flux in the 2–100 keV band will thus give the observed spectral index between $1.2 < \alpha < 2.2$. An alternative process of X-ray emission due to external Compton process has been discussed in literature (Dermer & Schlickeiser 1993). However, the correlation between the K-band and the X-ray data suggests a common origin of these photons. As noted earlier, the multifrequency observations of 3C273 do not show any apparent temporal correlation in various bands. This is probably due to the fact that the large majority of the hard X-ray and gamma ray photons originate in the radio jet while the soft X-ray excess, the blue bump in UV are due to the accretion disk.

5.2 *Long term period and the source geometry*

Any proposed geometrical model with possible sites and the mechanism of photon emission must also explain the long term period of $\sim$ 5000 days in 3C273 as discussed above. Long term periodicity of 23.1 ± 1.1 years for Mkn 421, 13.7 ± 1.3 year for ON 231, 12 years for OJ 287 and 6 years in the case of 3C345 have also been reported from the analysis of their optical data (Liu *et al.* 1995, 1997; Sillanpaa *et al.* 1988b; Unwin *et al.* 1997). Such times scales can only be associated with the activity of the central region of the host galaxy i.e., either the accretion disk or the central black hole system. The precession time scale in either case are too long to be observed and therefore, the observed periodic behaviour in 3C273 can only be explained either by the orbital period by assuming a binary black hole system in the center of the quasar or in terms of the thermal limit cycle (oscillations) time scale in slim accretion disk around the black hole, similar to the models suggested for other sources with long term variability (Sillanpaa *et al.* 1988a; Honma *et al.* 1991).

In the thermal limit cycle model, the nonlinear oscillations can originate in a thermally unstable region of the accretion disk, which are caused by the mass accretion rate above a critical limit. This model was first suggested to explain the bursts in dwarf novae and their S-curve behaviour (e.g., Ritter 1988; King *et al.* 1997,). These models have been extended to the accretion disks around neutron stars and black holes (Taam & Lin 1994; Matsumoto *et al.* 1989; Honma *et al.* 1991). In the thin disk models, the viscosity is the key factor which determines the stability of the inner parts of the

accretion disk since the instability may set in for certain value of viscous stress when it is proportional to the total pressure (Shakura & Sunyaev 1976). A variety of stability criteria for the inner regions of the disk have been proposed in literature (Tam & Lin 1984; Abramowicz 1981; Lasota 1989). It has been recently shown that a limit-cycle behaviour of thermal instability can indeed occur only if there exists a high temperature stable equilibria, wherein the inner regions of the disk transits between optically thin and optically thick geometry (Lasota & Pelat 1991). The burst cycle time in this model is given by (Honma *et al.* 1991);

$$t_{\rm cyc} \sim 2\, t_{\rm burst} \sim 5 \times 10^3\, \alpha_{0.1}^{-0.62}\, M_8^{1.37} \ \text{yrs.}$$

Assuming a typical value of $\alpha_{0.1} \sim 1$, the estimated mass of the central black hole necessary to obtain a long term period of 13.5 yrs is $M \simeq 10^6 M_\odot$. This value is two orders of magnitude smaller than the mass of the source required to explain the observed luminosity of the source.

We propose that central core of the 3C273 contains a super massive black hole binary system and the observed periodicity in the X-ray flux is due to the orbital period of the two components. The concept of super massive system of binary black holes in radio galaxies was first proposed by Begelman *et al.* (1980) to explain the observed precession of radio jets. Similarly, to explain the quasi-periodic behaviour of BL Lac OJ 287 in optical band and the radio features in 3C345, a binary black hole model has been proposed for these sources (Sillanpaa *et al.* 1988a; Lobanov & Roland 2002). The presence of a binary black hole system orbiting around their centre of mass in the AGNs, is likely to effect the gas dynamics in the accretion disk, which in turn will affect the gas emission features i.e., the broad emission lines (Begelman *et al.* 1980), narrow emission lines (Gaskell 1996) and even the Iron K_α emission line feature in the X-ray band (Yu & Lu 2001). There is a growing evidence of BBH systems in the active galactic nuclei. For example, observation double peaked Balmer lines of quasar OX 169 have been interpreted as due to binary black hole system (Stockton & Farnhem 1991). The observed complex line profile of 3C273 and its variability does support a binary black holes hypothesis for the source. A model involving a binary black hole system in circular orbit has also been invoked by Reiger and Manheim (2000) to explain the 23 day variability in Mkn 501, observed in the X-ray and TeV gamma rays energy bands (Protheroe *et al.* 1998; Hayashida *et al.* 1998; Nishikawa *et al.* 1999). While the implications of the generalized orbits for a binary black hole system are discussed by De Paolis *et al.* (2001). For a circular orbit, the orbital period P is given as (Yu & Lu 2001);

$$P \approx 210\, a_{0.1pc}^{3/2} \left(\frac{2\, M_8}{m_1 + m_2}\right)^{1/2} \ \text{yrs,}$$

where: $a_{0.1pc}$ is the distance between two black holes in units of 0.1 pc and M_8, is the mass unit $10^8 M_\odot$. Assuming a binary separation of 0.01 pc and the observed period of 13.5 yrs in 3C273, the $m_1 + m_2 \approx 0.5 \times 10^8 M_\odot$. Core mass of $\sim 10^8 M_\odot$ is consistent with the inferred Eddington mass limit for the observed luminosity of $\sim 10^{46}$ ergs s^{-1} from the source.

In summary, the hard X-ray spectrum in 3C273 consists of two components. First, the underlying synchrotron emission from the jet which extends from radio energies to GeV photons and has a steep power with $\alpha \sim 2.3$ as measured in the present data. The

second component consists of the disk emission which accounts for Iron K_α emission line and also contributes to continuum flux in the medium energy band. We have also presented evidence that the source exhibits a long term periodicity of 13.5 yrs, which is also present in the optical data of the source. We have also shown that the long term periodicity of the source can be explained by a binary black hole model for 3C273.

Acknowledgements

It is a great pleasure to acknowledge the support of the LASE team of J. A. R. D'Silva, P. P. Madhwani, N. V. Bhagat and Ms. N. Kamble for the fabrication of the payload and the successful balloon flight. I also thank Mr. S. Sreenivasan and the staff of the TIFR balloon facility at Hyderabad for the fabrication of the balloon and the successful balloon flight. BATSE and RXTE teams are gratefully acknowledged for making their data available on public archives. I sincerely thank Junhui Fan for providing the optical data of the source.

References

Abramowicz, M. A. 1981, *Nat.*, **294**, 235.
Bassani, L. *et al.* 1992, *Ap. J.*, **396**, 504.
Begelman, M. C., Blandford, R. D., Rees M. J., 1980, *Nat.*, **287**, 307.
Bezler, M., Kendziorra, E., Staubert, R. *et al.* 1984, *A & A*, **136**, 351.
Boyer, C. S., Lampton, M., Mack, J. 1970, *Ap. J.*, **161**, L1.
Courvoisier, T. J. L. *et al.* 1987, *A & A*, **176**, 21.
Cappi, M., Matsuoka, M., 1997, Proc. 2nd Integral workshop 'The Transparent Universe', (ed.) Winkler, Courvoisier & Durouchoucx, ESA, SP-382,
Cappi, M. and Matsuoka, M. Otani, M., Leighly, K. M. 1998, *PASJ*,
D'Silva, J.A.R. *et al.* 1998, *Nucl. Instrum. Methods*, **A412**, 34.
Damle, S. V., Kunte, P. K., Naranan, S. *et al.* 1987, *A & A*, **182**, L1.
Davis, R. J., Muxlow, T. W. B., Unwin, S. C. 1991, *Nat.*, **354**, 374.
Dean, A. J., Bazzano, A., Court, A. J. *et al.* 1990, *Ap. J.*, **349**, 41.
DePaolis, *et al.* 2002, *A & A*, **388**, 470.
Dermer, C. D., Schlickeiser, R. 1993, *Ap. J.*, **416**, 458.
Fan, J. H., Romero, G. E., Lin, R. G. 2001, *Acta Astronomica Sinica*, **42**, 9.
Gaskell, C. M. 1996, *Ap. J.*, **464**, L107.
Ginzberg, V. L., Syrovatskii, S. I. 1964, in *Origin of Cosmic Rays* (Pergamon Press)
Grandi, G. *et al.* 1997, *A & A*, **325**, L17.
Hayashida, N, Hirasawa, H., Ishikawa, F. *et al.* 1998, *Ap. J.*, **504**, L71.
Hermsen, W. *et al.* 1993, *A & A* **97**, 97.
Honma, F., Matsumoto, R., Kato, S. 1991, *PASJ*, **43**, 147.
Johnson, W.N. *et al.* 1995, *Ap. J.*, **445**, 182.
King, A. R., Frank, J., Kolb, U., Ritter, H. 1997, *Ap. J.*, **482**, 919.
Kim, C. 2001, *J. Astrophys. Astr.*, **22**, 283.
Konigl, A. 1981, *Ap. J.*, **243**, 700.
Lasota, J. P. 1989 In: (ed.) *Accretion disks and Magnetic fields in Astrophysics*, G. Belvedere, (Kluwer) p 273
Lasota, J. P., Pelat, D. 1991, *A & A*, **249**, 574.
Leach, C. M., McHardy, I. M., Papadakis, I. E., 1995, *MNRAS*, **272**, 221.
Litchi, G. G. *et al.* 1994, In: *The Second Compton Symposium*, (ed.) Fichtel, Gehrels & Norris, AIP, 611
Liu, F. K., Xie, G. Z., Bai, J. M. 1995, *A & A*, **295**, 1.
Liu, F. K., Liu, B. F., Xie, G. Z. 1997, *A & A*, **SS 123**, 569.

Lobanov, A. P., Roland, J. 2002, In: *Proc. 6th European VLBI network Symp.*, (ed.) Ross, Porcas, Labonov & Zensus, Bonn, p 121
Maisack, M. *et al.* 1989, *Proc. ESLAB Symp.*, **SP-296**, 975
Maisack, M., Kendziorra, E., Mony, B. *et al.* 1992, *A & A.* **262**, 433.
Manchanda, R. K. 1998, *Adv space Res.*, **21**, 1019.
Manchanda, R. K. 2001, *J. Astrophys. Astr.*, **22**, 145.
Maraschi, L. *et al.* 2000, *Adv. Space Res.*, **25**, 713.
Marshall, N., Warwick, R. S., Pounds, K. A. 1981, *MNRAS*, **194**, 987.
Matsumoto, R., Kato, S., Honma, F. 1989, In: *Theory of accretion disks*, (ed.) Meyer, Duschl, Frank and Meyer-Hofmeister, Kluwer, p 167
Mc Hardy, I., Lawson, A., Newsam, A. *et al.* 1999, *MNRAS*, **310**, 571.
Mitra, A. 1991, *Ap. J.*, **370**, 345.
Mushotzky, M. 1982, *Ap. J.*, **256**, 92.
Nishikawa, D., Hayashi, S. Chamoto, N. *et al.* 1999, *ICRC*, **3**, 26.
Pietsch, W., Reppin, C., Trumper, J. *et al.* 1981, *A & A*, **94**, 234.
Primini, F. A., Cooke, B. A., Dobson, C. A. *et al.* 1979, *Nat.*, **278**, 234.
Protheroe, J., Bhat, C. L., Fleury, P. *et al.* 1998, *ICRC*, **8**, 317.
Ramos, E., Kafatos, M., Fruscione, A. *et al.* 1997, *Ap. J.*, **482**, 167.
Reiger, F. M., Manheim, K. 2000, *A & A*, **359**, 948.
Ritter, H. 1988, *A & A*, **124**, 267.
Sambruna, R. M., Urry, C. M, Tavecchio, F. *et al.* 2001, *A & A*, **549**, L161
Shakura, N. I., Sunyaev, R. A. 1976, *MNRAS*, **175**, 613.
Sillanpaa, A., Haarala, S., Valtonen, M. J. 1988a, *et al. Ap. J.*, **325**, 628.
Sillanpaa, A., Haarala, S., Korhonen, T. 1988b, *A & A Suppl Ser.*, **72**, 347.
Stockton, A., Farnhem, T. 1991, *Ap. J.*, **368**, 28.
Storchi-Bergmann, T., Eracleous, M., Ruiz, M. T. *et al.* 1997, *Ap. J.*, **489**, 87.
Sunyaev, R. A., Titarchuck, L. G. 1980, *A & A*, **86**, 121.
Taam, R. E., Lin, D. N. C. 1984, *Ap. J.*, **287**, 761
Turner, M. J. L., Courvoisier, T., Staubert, R. *et al.* 1995, *Sp. Sci. Rev.*, **40**, 623.
Ulrich, M. H., Courvoisier, T. J. L., Warnsteber, W. 1988, *A & A*, **204**, 21
Unwin, S., Wehrle, A., Lobonov, A. P. *et al.* 1997, *Ap. J.*, **480**, 1997
von Montigny, C. *et al.* 1993, *A& A Suppl Ser.*, **97**, 101.
Warrell, D. M., Mushotzky, R. F., Boldt, E. A. *et al.* 1979, *Ap. J.*, **232**, 683.
Wilkes, B. J., Elvis, M. 1987, *Ap. J.*, **323**, 243,
Williams, O. R., Turner, M. J. L., Stewart, G. C. *et al.* 1992, *A & A.* **285**, 119.
Yu, Q., Lu, Y. 2001, *A & A*, **377**, 17.